HHS Public Access

Author manuscript

J Drug Target. Author manuscript; available in PMC 2020 June 01.

Published in final edited form as:

J Drug Target. 2019 ; 27(5-6): 582–589. doi:10.1080/1061186X.2018.1547732.

Transport and Delivery of Interferon-α Through Epithelial Tight Junctions via pH-Responsive Poly(Methacrylic Acid Grafted Ethylene Glycol) Nanoparticles

Mary Caldorera-Moore[1], **Julia E. Vela Ramirez**[2,3,4], and **Nicholas A. Peppas**[2,3,4,5,6,7,*]

[1]Department of Biomedical Engineering, Louisiana Tech University, Ruston, LA 71272

[2]McKetta Department of Chemical Engineering, The University of Texas at Austin, Austin, TX 78712, USA

[3]Department of Biomedical Engineering, The University of Texas at Austin, Austin, TX 78712, USA

[4]Institute for Biomaterials, Drug Delivery, and Regenerative Medicine, The University of Texas at Austin, Austin, TX 78712, USA

[5]Department of Surgery and Perioperative Care, Dell Medical School, The University of Texas at Austin, Austin, TX 78712, USA

[6]Department of Pediatrics, Dell Medical School, The University of Texas at Austin, Austin, TX 78712, USA

[7]Division of Molecular Pharmaceutics and Drug Delivery, College of Pharmacy, The University of Texas at Austin, Austin, Texas 78712, USA

Abstract

Whereas significant advancements have been made in our fundamental understanding of cancer, they have not yet translated into effective clinical cancer treatments. One of the areas that has the potential to improve the efficacy of cancer therapies is the development of novel drug delivery technologies. In particular, the design of pH-sensitive polymeric complexation hydrogels may allow for targeted oral delivery of a wide variety of chemotherapeutic drugs and proteins. In this work, poly(methacrylic acid grafted ethylene glycol) (P(MAA-g-EG) hydrogel nanoparticles were synthesized, characterized, and studied as matrix-type, diffusion-controlled, pH-responsive carriers to enable the oral delivery of the chemotherapeutic agent Interferon Alpha (IFN-α). The biophysical mechanisms controlling the transport of IFN-α were investigated using a Caco-2/HT29-MTX co-culture as a gastrointestinal (GI) tract model. The synthesized nanoparticles exhibited pH-responsive swelling behavior and allowed the permeation of IFN-α through the tight junctions of the developed cellular gastrointestinal epithelium model. These studies demonstrate the capabilities of these particles to contribute to the improved oral delivery of protein chemotherapeutics.

[*]**Corresponding Author:** Nicholas A. Peppas, Full Address: Department of Biomedical Engineering, The University of Texas at Austin, 107 W Dean Keeton Stop C0800, Austin, TX 78712, USA, Fax: (512) 471-8227, peppas@che.utexas.edu Phone: (512) 471-6644.

Keywords

Responsive Hydrogels; pH-Sensitive Hydrogel Nanoparticles; Interferon Alpha (IFN-α); GI Tract Delivery Systems; Caco-2 cell lines

Introduction

Advances in detection and tumor treatment have helped to reduce the number of deaths associated with many cancer types. Further improvements in patient survival can be aided through the development of new technologies to enhance the delivery of chemotherapeutic agents [1, 2, 3, 4, 5, 6]. While intravenous administration is currently the delivery method most prominently used in the clinic, a promising alternative is the oral administration of chemotherapeutics due to the comparable or improved efficacy, increased patient compliance, and lower cost [5, 7, 8].

Recent studies have indicated advantageous results following the oral delivery of chemotherapeutic agents when compared to intravenous administration [9, 10, 11, 12, 13, 14]. *In vivo* studies performed by Ren et al. [15] demonstrated that the oral delivery of cabazitaxel using nanocarriers with a hybrid core comprised of poly(ε-caprolactone) and medium-chain triglycerides with a positively charged surface using a polyethylene oxide shell induced tumor inhibition more effectively and caused less systemic toxicity compared with drug administered intravenously. The advantages to oral chemotherapy go beyond survival time and toxicity; lower treatment cost, increase patient compliance, flexibility of dosing schedule and an overall improvement in quality of life are additional benefits of oral chemotherapy [10].

Despite all of these advantages there are only a few oral chemotherapeutic drugs currently in clinical use. This is mainly due to the challenges of achieving efficacious drug concentration in the bloodstream [10]. This is especially difficult for small molecule drugs and protein chemotherapeutics like interferons, which are used as a treatment for a variety of cancers [16, 17, 18, 19]. For example, studies have shown that relatively high doses of IFN-α are necessary to elicit therapeutic responses in cancer patients; however, these regimens are highly toxic [20]. Due to its toxicity levels, IFN-α has been progressively phased out of clinical use [21, 22, 23, 24]. Therefore, the overall limited therapeutic use of current treatments based on IFN-α might reflect our inability to target these potent antitumor molecules to the right place and/or at the right dose. Alternative delivery strategies are thus needed to achieve safe and effective IFN delivery in cancer patients [25]. To accomplish this, a variety of different delivery systems have been explored for the delivery of IFN-α including the synthesis of PEGylated- IFN-α [26], encapsulation of IFN-α into poly(lactic-co-glycolic acid) (PLGA) microspheres [27], via microporation for transdermal delivery [28], and using a nanochannel delivery system [29]. While these approaches showed promising results they all lacked the ability to controlled release IFN-α and in the case of the nanochannel device, it required implantation at the tumor site.

The GI tract presents harsh and complex environments that make the oral administration of drugs challenging. These molecules are exposed to the harsh acidic environment of the

stomach and subject to the action of degradative enzymes in the GI tract. Additionally, the drug molecules have to be transported across biological barriers before they can reach the bloodstream, which may restrict their bioavailability or damage their stability. Furthermore, there is potential toxic effects on the GI tissue by the therapeutic agent, if high doses are necessary. Current research efforts are focused on understanding the biophysical mechanisms regulating oral administration of biopharmaceutics and on the development of better drug carrier systems to overcome these challenges.

For almost twenty five years, we have investigated intelligent, highly biocompatible carrier systems that can protect and deliver therapeutic agents, especially proteins, to their site of action [30, 31, 32, 33, 34]. For these systems to be effective, they also need to enable drug transport to the bloodstream, via a series of paracellular or transcellular mechanisms through the intestinal wall. The pH shift between the stomach and the upper small intestine can be used to our advantage to achieve the controlled release of drugs. Previously, our group has reported the development of a suite of intelligent, biocompatible micro- and nanocarrier systems that can protect a variety of therapeutic agents from the harsh environment in the stomach while also transporting the drug for site-specific release into the bloodstream in the upper small intestine [35, 36]. The developed matrix-type, diffusion-controlled carrier systems are composed of polymeric hydrogel materials that are complexation controlled and can be easily tailored to react to environmental cues [7, 37, 38]. Responsive hydrogels composed of ionic networks can be molecularly designed to swell in response to pH changes. By incorporating acidic or basic groups into the hydrogel networks with specific pKa (acid dissociation constant of a specific molecule) the hydrogels can be tailored to swell at specific pH values [39, 40, 41, 42].

In this work, poly(methacrylic acid- grafted- ethylene glycol) hydrogel nanoparticles were prepared to create pH responsive, matrix-type carriers for oral delivery of the protein-based chemotherapeutic agent IFN-α. Using these particles, we investigated the biophysical mechanisms controlling the permeability of IFN-α for cancer treatment. To accomplish this, a co-culture monolayer model of human epithelial colorectal adenocarcinoma cells (Caco-2) and HT29-MTX human colon carcinoma cells was employed as previously reported by our group [43, 44].

Materials and Methods

Nanocarrier Synthesis—Poly(methacrylic acid)- grafted- poly(ethylene glycol) methyl ether methacrylate – co- *tert*-butylamino methacrylate], designated henceforth as (P(MAA-g-EG-co-tBMA)), complexation hydrogels were synthesized by a photo-emulsion polymerization method previously reported by our group [36]. Briefly, *tert*-butylamino methacrylate (t-BMA, Sigma-Aldrich, St. Louis, MO), and tetra(ethylene glycol) dimethacrylate (TEGDMA, Sigma-Aldrich, St. Louis, MO) were passed through a column of basic alumina powder to remove inhibitor prior to use. Methacrylic acid (MAA, St. Louis, MO) was vacuum distilled at 54 °C/25 mm Hg to remove the inhibitor, and poly(ethylene glycol) methyl ether methacrylate ((PEGMMA), Mn ~ 2080, Sigma-Aldrich, St. Louis, MO) was used as received.

Crosslinker and monomer were added to an aqueous solution of 5 wt.% PEGMMA, Irgacure 2959 (Ciba Geigy, Basel, Switzerland) at 0.5 wt.% of total monomer. The ionic surfactants Brij-30 (Acros Organics, Morris, NJ) and sodium dodecyl sulfate (SDS) (Fisher Bioreagents, Pittsburgh, PA) were added to the precursor solution to stabilize the emulsion at 4 mg mL^{-1} and 8.2 mM, respectively. The mixture was emulsified using a Misonix Ultrasonicator (Misonix, Inc., Farmingdale, NY).

The emulsion was purged with nitrogen gas for 20 minutes and exposed to UV light (Dymax, BlueWave200 UV, Torrington, CT) for 2.5 h with constant stirring. Surfactants and unreacted monomers were removed by repeatedly inducing polymer-ionomer collapse, separating particles by centrifugation, and resuspending in 0.5 N NaOH. Polymer particles were dialyzed against deionized water (DI H_2O) for 7 days with twice daily water changes. The particles were then freeze-dried and stored until further use.

Nanoparticle Characterization

Scanning Electron Microscopy—SEM micrographs of synthesized and lyophilized particle samples were collected using a Zeiss Supra 40 VP scanning electron microscope. Samples were coated with an 8 nm layer of Pt-Pd immediately prior to imaging.

Dynamic Light Scattering (DLS)—Dynamic light scattering (DLS) studies were used to verify the hydrodynamic diameter of the synthesized nanoparticles as the particles were subject to an increase in pH. The hydrodynamic diameter of the polymer networks was measured in aqueous suspension using a Malvern Zetasizer NanoZS (Malvern Instruments Corp., Malvern, UK) operating with a 633 nm laser source equipped with a MPT-2 Autotitrator. DLS measurements of particle size and pH- responsive behavior were conducted by resuspending lyophilized particles in PBS at 0.5 mg mL^{-1}. The suspension pH was adjusted from pH 4.5 to 8.5 using 1 N NaOH. Measurements of the Z-average particle size were collected at 25 °C using pH intervals of 0.5.

Electrophoretic light scattering—The effective surface ζ-potential of the polymer networks was measured using a Malvern Zetasizer NanoZS (Malvern Instruments Corp., Malvern, UK) operating with a 633 nm laser source equipped with a MPT-2 Autotitrator. Measurements of ζ-potential as a function of pH were conducted by resuspending lyophilized particles in 5 mM phosphate buffer at 0.5 mg/mL. The suspension pH was adjusted from pH 4.5 to 8.5 using 1 N NaOH. Electrophoretic light scattering measurements of the surface ζ- potential were collected at 25 °C.

Loading studies—Loading efficiency studies were conducted to evaluate the capability to encapsulate recombinant human IFN-α (alpha 2A, Pestka Biomedical Laboratories (PBL) Assay Science, Piscataway, NJ) by the synthesized P(MAA-g-EG-co-*t*BMA) nanoparticles. Briefly, P(MAA-g-EG-co-*t*BMA) nanoparticles (0.5 mg mL^{-1}) were incubated in PBS at pH 7.4 for 24 hours to fully swell the hydrogel network. IFN-α was then introduced to the nanoparticle solution at a final concentration of 0.05 μg of protein mg^{-1} of particles and incubated for 1 hour before the particle networks were collapsed by dropping the solution pH to 4.6. The nanoparticles were then rinsed 3 times in fresh PBS at pH 4.8. The amount of

IFN-α remaining in the supernatant following the 1-hour incubation, after collapse, and particle rinses was measured using a VeriKine™ Human IFN-α ELISA Kit (PBL Assay Science).

In Vitro Performance Characterization

In vitro characterization of the biocompatibility and ability to effectively transport IFN-α across the intestinal lining of the developed particles was determined using a Caco-2/HT29 MTX co-culture model previously reported by the Peppas lab [43]. Caco-2 cells were obtained for the American Type Culture Collection (ATCC, Manassas, VA) and HT29-MTX cells were generously donated by Dr. Thecla Lesuffleur (INSERM, Paris, France). HT29-MTX cells are a sub-population of HT29 cells that were adapted to 10^{-6} M methotrexate (MTX) [45, 46].

All cell types were cultured in Dulbecco's Modified Eagle Medium (DMEM) high glucose supplemented with 10% heat-inactivated fetal bovine serum, with 1% streptomycin from Sigma Life Sciences (St. Louis, MO). Dulbecco's Phosphate-Buffered Saline (DPBS) and was also obtained from Sigma Life Sciences (St. Louis, MO). Individual cultures of the Caco-2 and HT-29 MTX cells were maintained in T-75 flasks at 37°C and 5% CO_2. The culture medium was changed every 48 hours. Cells were consistently passaged at 80% confluence, which occurred between 6 and 7 days after seeding. A passage consisted of two washes with Dulbecco's phosphate buffered saline (DPBS) without Ca^{2+} and Mg^{2+}, followed by the addition of 1 ml of 0.5% trypsin/0.2% EDTA solution with a 5–8 min incubation after which cells were detached from the flasks and could then be counted and reseeded. Caco-2 cells were seeded at a density of 3.0×10^3 cells cm^{-2} and used between passages 60 and 80. HT29–MTX cells were seeded at a density of 2.0×10^4 cells cm^{-2} and used between passages 8 and 20.

Biocompatibility studies—Cytocompatibility of the synthesized nanocarriers was investigated using a cellular metabolic assay CellTiter 96® Aqueous One Solution Cell Proliferation Assay (Promega, Madison, WI). Human epithelial colorectal adenocarcinoma cells (Caco-2) were incubated with various concentrations of purified P(MAA-g-EG-co-tBMA) nanoparticles for 2 hours. After the incubation period, the effect of particles on cellular proliferation was quantified. Replicates of 6 for each data point were used.

IFN-α transport studies—Transport studies were conducted as previously reported by our group using Costar Transwell® plates with a polycarbonate membrane (0.4 μm pore size) and a 1 cm^2 cell growth area (12 well plates) [43]. Caco-2 and HT29-MTX cells were seeded on the apical side of Transwell® plates at a 1:1 ratio at a final cell density of 6×10^5 cells cm^{-2}; which has been shown previously to produce transepithelial electrical resistance (TEER) values that closely match reported *in vivo* values for human intestinal epithelia [43, 44]. Cell culture media was changed every other day in both the apical and basolateral sides of the Transwell® plates.

Transepithelial electrical resistance was used to evaluate the formation of tight junctions in the Transwell® co-cultures. Measurements were taken every other day, 2 hours after media changes using an EVOM volt-ohm meter and a chopstick electrode (World Precision

Instruments, Sarasota, FL). In order to calculate the resistance across the cellular monolayer, it was necessary to subtract out the resistance from the membrane and the media in the wells. Blank resistance measurements for every well was taken in the presence of complete DMEM media prior to seeding the cells. The measured blank resistance values were then subtracted from the experimental TEER value. During the TEER measurements, Transwell® plates were placed on a heating mat to maintain the temperature at 37 °C.

Transport studies were performed to determine the amount of IFN-α across a cellular monolayer with and without the presence of the P(MAA-g-EG-co-*t*BMA) nanoparticles. Passage 70 Caco-2 cells and passage 14 HT29–MTX cells were cultured in a 12-well Transwell® plates for 24 days as previously described. To prevent IFN-α from adhering to the Transwell® plates during the transport studies, the plates were first blocked with bovine serum albumin (BSA) (Sigma-Aldrich, St. Louis, MO) prior to introducing IFN-α. A 0.5 mg mL^{-1} BSA solution in Hank's balanced salt solution (HBSS, Thermo Scientific, Waltham, MA) was used. The solution was then filtered using a GE Healthcare Whatman™ 0.02 μm anotop filter (Fisher Scientific, Waltham, MA) and pre-warmed for 20 minutes at 37°C. Cell culture media was removed from the apical and basolateral chambers and replaced with pre-warmed BSA-HBSS solution after first washing both chambers one time with HBSS. The BSA-HBSS in both the apical and basolateral chambers contained Ca^{2+} at a concentration of 1.26 mM. Cells were allowed to equilibrate for one hour and TEER measurements were taken at 0 and after 1 hour. For all samples and TEER measurements the Transwell® plates were placed on a heating mat to maintain the temperature at 37 °C.

IFN-α was dissolved at a concentration of 0.0012 mg mL^{-1} diluted in the BSA-HBSS solutions. IFN-α solutions were warmed at 37 °C for 15 minutes prior to addition to the equilibrated cells. For samples containing nanoparticles, the nanoparticles were added to the IFN-α solution at a concentration of 1 mg mL^{-1} immediately before adding the sample to the apical chamber. Control wells contained only the IFN-α/BSA/HBSS solution without nanoparticles. After sample addition, 0.1 mL IFN-α samples were taken from the apical chamber at 0 and 3 hours and from the basolateral chamber at 0, 0.5, 1, 2, and 3 hours. Samples were replaced with a pre-warmed HBSS solution containing 0.5 mg mL^{-1} BSA. TEER values were monitored over the course of the experiment. After 3 hours, the contents of the apical chamber were removed and washed 2 times with HBSS. Fresh, pre-warmed cell culture media was then added to both the apical and basolateral chambers and TEER values were monitored over the next 24 hours.

IFN-α concentration was determined using the VeriKine™ Human IFN-α ELISA Kit (PBL Assay Science, Piscataway, NJ). The high sensitivity range of the kit was 12.5–500 pg mL^{-1} and the extended range of the ELISA was 156–5000 pg mL^{-1}. The apparent permeability coefficient P_{app}, was calculated from the following equation:

$$P_{app} = \left(\frac{dQ}{dt}\right)\frac{1}{A \bullet C_0}$$

Where dQ/dt represents the steady-state flux of IFN-α across the cell monolayer, A is the surface area of the membrane, and C_0 is the initial IFN-α concentration in the apical

chamber. The flux across the cell monolayer was calculated from the slope of the IFN-α transport to the basolateral chamber versus time.

Results and Discussion

Poly(methacrylic acid-grafted-poly(ethylene glycol) methyl ether methacrylate-co-*t*-Butylamino methacrylate (*t*BMA) (P(MAA-*g*-EG-co-tBMA)) complexation hydrogel nanoparticles were synthesized and evaluated as an oral drug delivery system for the protein chemotherapeutic agent interferon alpha (IFN-α). Nanoparticle size was determined using scanning electron microscopy and dynamic light scattering. The pH responsiveness and zeta potential of the developed carriers were also determined using dynamic light scattering under different conditions. A series of studies were conducted to evaluate the properties and *in vitro* performance of the fabricated nanogels as an oral drug delivery system (DDS).

Nanoparticle Characterization

Nanoparticle size was determined using scanning electron microscopy and dynamic light scattering. Electron micrographs obtained from dry samples were used to qualitatively evaluate the size, shape, and polydispersity of the nanoparticles (Figure 1). Figure 1A shows the morphology of the carriers after synthesis, purification, and dialysis. These findings confirm that the aqueous photo-emulsion nanoparticle synthesis method produced nanoscale spherical particles (~460 nm in diameter), consistent with previous reports [47]. Following lyophilization the particle size was reduced to ~80 nm as shown in Figure 1B.

Size and zeta potential of the produced hydrogels were confirmed using dynamic light scattering. DLS measurements of particle size were conducted as a function of pH using an auto-titration system, confirming their pH- responsive behavior. As shown in Figure 2A an increase in particle diameter from 103.1 nm to 134.5 nm was observed when the solution pH was increased above 5 which is close to the pKa of MAA. A swelling transition at pH 5 indicates that drug release as a result of decomplexation would occur in the upper small intestine [47, 48]. Measurements of the effective surface ζ-potential of the P(MAA-g-EG-co-*t*BMA) nanoparticles revealed a decrease in charge at pH 5 when the particles being to swell (Figure 2B).

Loading efficiency studies were then conducted to evaluate the capability of P(MAA-g-EG-co-tBMA) nanoparticles to encapsulate recombinant human IFN-α. Nanoparticles were incubated for 1 hour in an IFN-α solution prior to collapsing the hydrogel network to effectively encapsulate the IFN-α. After the 1-hour incubation period, 60.4% of the IFN-α was encapsulated or attached to the surface of the nanoparticles (Table 1). After collapsing and rinsing the hydrogel network the final percent loading was determined to be 37.4%. These amounts are comparable to the obtained with other delivery platforms [49].

In Vitro Characterization Biocompatibility

To evaluate the biocompatibility of the synthesized carriers, cytocompatibility studies were conducted using an MTS assay, which monitors the mitochondrial activity of the cells. The results from the cytotoxicity evaluation (Figure 3) show that the P(MAA-g-EG-co-*t*BMA) nanoparticles with 1% (w/w) TEGDMA crosslinker (1X) and 3% (w/w) TEGDMA

crosslinker (3X) were non-toxic to the cells at 1, 2.5 and 5 mg mL^{-1} concentrations. The concentration of the nanoparticles did not affect the particle toxicity although there was a decrease in cell proliferation observed with the higher crosslink concentration at the 5 mg mL^{-1} concentration. These results are consistent with previously developed hydrogel platforms from our group [48].

IFN-a Transport Studies Using Cell Lines

The Caco-2 cell line is a continuous line of heterogeneous human epithelial colorectal adenocarcinoma cells; and since the 1990s monolayers of Caco-2 cells have become the gold standard for investigating the permeability of therapeutic drugs [50, 51]. Caco-2 cells are derived from a colon (large intestine) carcinoma and when cultured under specific conditions the cells became differentiated and polarized. Their phenotype, morphologically and functionally, resembles the enterocytes lining the small intestine. In addition, Caco-2 cells express tight junctions, microvilli, and a number or enzymes and transporters that are characteristic of enterocytes like: peptidases, esterases, and P-glycoproteins [50, 52].

One limitation of the model is that Caco-2 cells only differentiate into absorptive enterocytes, whereas the intestinal epithelial layer consists of a variety of different cell types, including goblet cells (mucus-secreting), enteroendocrine cells and M-cells. Due to the lack of goblet cells, there is no mucus layer lining the cellular monolayer. For this reason, a variety of different cell lines have been investigated to develop a mucus producing intestinal epithelial layer model. One such cell line is the human colon carcinoma HT29 cells that are both columnar absorptive and mucus secreting cells. Various sub clones of this cell line that differentiate into predominantly mucus secreting cells have been developed including the HT29-H [53, 54, 55] and HT29-MTX [52, 56, 57] cells. HT29-MTX cells are a sub-population of HT29 cells that were adapted to 10^{-6} M methotrexate (MTX) that develop an apical brush border which strongly expresses dipeptidylpeptidase IV, carcinoembryonic antigen, and villin [45, 46]. Previously, our group has worked on the optimization of the Caco-2 gastrointestinal (GI) model with the addition of HT29-MTX cells into the model [43]. A co-culture of Caco-2/HT29 cells creates a GI tract model that produces enzymes and mucus, possess tight junctions, and will develop microvilli.

IFN-α transport studies were conducted to examine the difference in transport of drug from nanoparticle versus free IFN-α across a Caco-2 and HT29-MTX co-culture cell monolayer model. Transepithelial electrical resistance (TEER) was employed to evaluate the development of tight junctions within the cellular monolayer. This evaluation has been used to measure drug permeability and for the selection of leading formulations [58, 59]. To produce a cell monolayer with TEER values close to that of human intestinal epithelia, cells were cultured for 24-days. Phase contrast images of the co-culture over time (Figure 4) shows that by day 7 (Figure 4B) a cell monolayer is formed. By day 21, large amounts of mucus from the HT29-MTX cells are visible to the point that it is hard to see the monolayer of cells underneath (Figure 4D). This co-culture has shown to present similar morphofunctional properties as an in vitro model of human intestinal epithelium [60]. The monolayer morphology and TEER measurements confirm the success establishing the *in*

vitro model and the suitability of this model to determine the capability of the developed delivery vehicles to induce IFN-α transport across the epithelium.

The TEER of the monolayer was measured every other day over the 24-day period (Figure 5A**)**. Additionally, the TEER was monitored during the IFN-α studies (Figure 5B). No significant drop in the cell monolayer resistances was observed during the incubation of the cells with either free IFN-α or the P(MAA-g-EG-co-tBMA) nanoparticles with IFN-α. To determine the amount of drug transported across the cell monolayer, samples were taken at different time points during the experiment and protein concentration was determined using IFN-α ELISA kit as shown in Figure 6. For all samples, the IFN-α permeability (P_{app}) was calculated (Table 2). The P_{app} for the IFN-α and nanoparticles sample (n=4) set was marginally higher but not statistically significantly different from the free IFN-α samples ($p = 0.2150$). These results demonstrate that the developed nanoparticles do not hinder transport of IFN-α across the co-culture monolayer. However, the tight junctions are composed of transmembrane and cytosolic proteins that prevent the diffusion of large molecules, thus the limited transport of free IFN-α. In previous studies, the presence of polymeric formulations has been shown to induce a permeation enhancement effect in gastrointestinal epithelium cellular models, as demonstrated by Sadeghi et al. [61]. Furthermore, there are variations in the tight junction present along the small intestine, which may cause that IFN-α transport to be higher *in vivo* than in the co-culture model [62].

Overall, these findings demonstrate that the developed P(MAA-g-EG-co-tBMA) nanoparticles have the potential to be used as an oral delivery system capable of protecting the IFN-α in the acidic environment of the stomach while allowing for the controlled release of the protein in the upper small intestine, and its transport across the intestinal lining at comparable concentrations than free IFN-α.

Conclusions

In this work we have demonstrated the ability to synthesize pH-responsive, hydrogel nanocarriers for the oral delivery of IFN-α. SEM and DLS were used to confirm the formation of spherical nanoparticles that swell as the environmental pH increases from acidic to neutral. Loading efficiency of IFN-α in the synthesized P(MAA-g-EG-co-tBMA) nanoparticles was determined to be 37.4%. Cytocompatibility studies confirmed that the developed nanoparticles did not cause detrimental effects to Caco-2 cells. IFN-α transport studies were conducted to examine the differences between IFN-α loaded nanoparticles versus free IFN-α across a Caco-2 and HT29-MTX co-culture cell monolayer model. Transepithelial electrical resistance (TEER) was employed to evaluate the development of tight junctions within the cellular monolayer and their maintenance during the IFN-α transport studies. No significant drop in the resistance of the cell monolayer was observed during the incubation of the cells with either free IFN-α or in the presence of IFN-α within P(MAA-g-EG-co-tBMA) nanoparticles. These results further confirm the suitability of the developed nanocarriers for the oral delivery of proteins. The values of P_{app} for the nanoparticles-loaded with IFN-α were higher but did not show statistically significance when compared to the free IFN-α groups; demonstrating that the developed nanoparticles support the transport of IFN-α across the co-culture monolayer. Ultimately, these carriers

will allow for sensitive protein chemotherapeutic agents to be efficiently delivered via the oral route, therefore eliminating the need of systemic IV administration.

Acknowledgements

This work was supported in part by grant U54-143837-02 from the US National Institutes of Health (NIH) and by the Pratt Foundation and the Cockrell Foundation. This work is dedicated to Professor Patrick Couvreur of the University of Paris-Sud who has been a strong academic and personal friend of Prof. N. A. Peppas since 1980.

We are honoring Patrick Couvreur for his sustained and outstanding scientific achievements in drug delivery and targeting and we rejoice on his recognition by the Journal's Lifetime Achievement Award for 2019. Since the publication in 1988 of their work on alginate magnetic releasing systems, Drs. Couvreur and Peppas have worked on the development and improvement of systems for protein delivery using a range of administration routes. Congratulations for 40 years of great research.

References

1. Couvreur P, Vauthier C. Nanotechnology: Intelligent Design to Treat Complex Disease. Pharmaceut Res. 2006 2006/7/01;23(7):1417–1450. doi: 10.1007/s11095-006-0284-8.
2. Nicolas J, Mura S, Brambilla D, et al. Design, functionalization strategies and biomedical applications of targeted biodegradable/biocompatible polymer-based nanocarriers for drug delivery. Chemical Society Reviews. 2013;42(3):1147–1235. doi: 10.1039/C2CS35265F. [PubMed: 23238558]
3. Spencer DS, Puranik AS, Peppas NA. Intelligent nanoparticles for advanced drug delivery in cancer treatment. Current Opinion in Chemical Engineering. 2015 2015/2/01/;7:84–92. doi: 10.1016/j.coche.2014.12.003.
4. Langer R, Peppas NA. Advances in biomaterials, drug delivery, and bionanotechnology. AIChE Journal. 2004 2003/12/01;49(12):2990–3006. doi: 10.1002/aic.690491202.
5. Liechty WB, Peppas NA. Expert opinion: Responsive polymer nanoparticles in cancer therapy. European Journal of Pharmaceutics and Biopharmaceutics. 2012 2012/2/01/;80(2):241–246. doi: 10.1016/j.ejpb.2011.08.004.
6. Steichen SD, Caldorera-Moore M, Peppas NA. A review of current nanoparticle and targeting moieties for the delivery of cancer therapeutics. European Journal of Pharmaceutical Sciences. 2013 2013/2/14/;48(3):416–427. doi: 10.1016/j.ejps.2012.12.006.
7. Blanchette J, Peppas NA. Oral Chemotherapeutic Delivery: Design and Cellular Response. Annals of Biomedical Engineering. 2005 2005/2/01;33(2):142–149. doi: 10.1007/s10439-005-8973-8.
8. Caldorera-Moore ME, Liechty WB, Peppas NA. Responsive Theranostic Systems: Integration of Diagnostic Imaging Agents and Responsive Controlled Release Drug Delivery Carriers. Accounts of chemical research. 2011 9/20;44(10):1061–1070. doi: 10.1021/ar2001777. [PubMed: 21932809]
9. Luo C, Sun J, Du Y, et al. Emerging integrated nanohybrid drug delivery systems to facilitate the intravenous-to-oral switch in cancer chemotherapy. Journal of Controlled Release. 2014 2014/2/28/;176:94–103. doi: 10.1016/j.jconrel.2013.12.030.
10. Thanki K, Gangwal RP, Sangamwar AT, et al. Oral delivery of anticancer drugs: Challenges and opportunities. Journal of Controlled Release. 2013 2013/8/28/;170(1):15–40. doi: 10.1016/j.jconrel.2013.04.020.
11. Mei L, Zhang Z, Zhao L, et al. Pharmaceutical nanotechnology for oral delivery of anticancer drugs. Advanced Drug Delivery Reviews. 2013 2013/6/15/;65(6):880–890. doi: 10.1016/j.addr.2012.11.005.
12. Mazzaferro S, Bouchemal K, Ponchel G. Oral delivery of anticancer drugs I: general considerations. Drug Discovery Today. 2013 2013/1/01/;18(1):25–34. doi: 10.1016/j.drudis.2012.08.004.
13. Mazzaferro S, Bouchemal K, Ponchel G. Oral delivery of anticancer drugs II: the prodrug strategy. Drug Discovery Today. 2013 2013/1/01/;18(1):93–98. doi: 10.1016/j.drudis.2012.08.006.

14. Mazzaferro S, Bouchemal K, Ponchel G. Oral delivery of anticancer drugs III: formulation using drug delivery systems. Drug Discovery Today. 2013 2013/1/01/;18(1):99–104. doi: 10.1016/j.drudis.2012.08.007.
15. Ren T, Wang Q, Xu Y, et al. Enhanced oral absorption and anticancer efficacy of cabazitaxel by overcoming intestinal mucus and epithelium barriers using surface polyethylene oxide (PEO) decorated positively charged polymer-lipid hybrid nanoparticles. Journal of Controlled Release. 2018 2018/1/10/;269:423–438. doi: 10.1016/j.jconrel.2017.11.015.
16. Bracci L, Schiavoni G, Sistigu A, et al. Immune-based mechanisms of cytotoxic chemotherapy: implications for the design of novel and rationale-based combined treatments against cancer [Review]. Cell Death And Differentiation. 2013 6/21/online;21:15. doi: 10.1038/cdd.2013.67. [PubMed: 23787994]
17. Motzer RJ, Bacik J, Murphy BA, et al. Interferon-Alfa as a Comparative Treatment for Clinical Trials of New Therapies Against Advanced Renal Cell Carcinoma. Journal of Clinical Oncology. 2002 2002/1/01;20(1):289–296. doi: 10.1200/JCO.2002.20.1.289.
18. Goldstein D, Laszlo J. The role of interferon in cancer therapy: A current perspective. CA: A Cancer Journal for Clinicians. 1988 1988/9/01;38(5):258–277. doi: 10.3322/canjclin.38.5.258.
19. Vela L, Marzo I. Bcl-2 family of proteins as drug targets for cancer chemotherapy: the long way of BH3 mimetics from bench to bedside. Current Opinion in Pharmacology. 2015 2015/8/01/;23:74–81. doi: 10.1016/j.coph.2015.05.014.
20. Parker BS, Rautela J, Hertzog PJ. Antitumour actions of interferons: implications for cancer therapy [Review Article]. Nature Reviews Cancer. 2016 2/25/online;16:131. doi: 10.1038/nrc.2016.14 [PubMed: 26911188]
21. Belardelli F, Ferrantini M, Proietti E, et al. Interferon-alpha in tumor immunity and immunotherapy. Cytokine & Growth Factor Reviews. 2002 2002/4/01/;13(2):119–134. doi: 10.1016/S1359-6101(01)00022-3.
22. Brassard DL, Grace MJ, Bordens RW. Interferon-α as an immunotherapeutic protein. Journal of Leukocyte Biology. 2002 2002/4/01;71(4):565–581. doi: 10.1189/jlb.71.4.565.
23. Gutterman JU. Cytokine therapeutics: lessons from interferon alpha. Proceedings of the National Academy of Sciences of the United States of America. 1994;91(4):1198–1205. [PubMed: 8108387]
24. Parmar S, Platanias LC. Interferons: mechanisms of action and clinical applications. Current Opinion in Oncology. 2003;15(6):431–439. [PubMed: 14624225]
25. Xu D, Smolin N, Shaw RK, et al. Molecular insights into the improved clinical performance of PEGylated interferon therapeutics: a molecular dynamics perspective. RSC Advances. 2018;8(5):2315–2322. doi: 10.1039/C7RA12480E.
26. Micco L, Peppa D, Loggi E, et al. Differential boosting of innate and adaptive antiviral responses during pegylated-interferon-alpha therapy of chronic hepatitis B. Journal of Hepatology. 2013;58(2):225–233. doi: 10.1016/j.jhep.2012.09.029. [PubMed: 23046671]
27. Sánchez A, Tobío Ma, González L, et al. Biodegradable micro- and nanoparticles as long-term delivery vehicles for interferon-alpha. European Journal of Pharmaceutical Sciences. 2003 2003/3/01/;18(3):221–229. doi: 10.1016/S0928-0987(03)00019-8.
28. Badkar AV, Smith AM, Eppstein JA, et al. Transdermal Delivery of Interferon Alpha-2B using Microporation and Iontophoresis in Hairless Rats. Pharmaceutical Research. 2007 2007/7/01;24(7):1389–1395. doi: 10.1007/s11095-007-9308-2.
29. Lesinski GB, Sharma S, Varker KA, et al. Release of Biologically Functional Interferon-Alpha from a Nanochannel Delivery System. Biomedical Microdevices. 2005 2005/3/01;7(1):71–79. doi: 10.1007/s10544-005-6174-8.
30. O'Connor C, Steichen S, Peppas NA. Student Award for Outstanding Research Winner in the Undergraduate Category for the 2017 Society for Biomaterials Annual Meeting and Exposition, April 5–8, 2017, Minneapolis, Minnesota: Development and characterization of stimuli-responsive hydrogel microcarriers for oral protein delivery. Journal of Biomedical Materials Research Part A. 2017 2017/5/01;105(5):1243–1251. doi: 10.1002/jbm.a.36030.

31. Horava SD, Moy KJ, Peppas NA. Biodegradable hydrophilic carriers for the oral delivery of hematological factor IX for hemophilia B treatment. International Journal of Pharmaceutics. 2016 2016/11/30/;514(1):220–228. doi: 10.1016/j.ijpharm.2016.05.056.
32. Lowman AM, Morishita M, Kajita M, et al. Oral delivery of insulin using pH-responsive complexation gels. Journal of Pharmaceutical Sciences. 1999 1999/9/01/;88(9):933–937. doi: 10.1021/js980337n.
33. Morishita M, Goto T, Nakamura K, et al. Novel oral insulin delivery systems based on complexation polymer hydrogels: single and multiple administration studies in type 1 and 2 diabetic rats. Journal of controlled release : official journal of the Controlled Release Society. 2006;110(3):587–594. doi: 10.1016/j.jconrel.2005.10.029. [PubMed: 16325951]
34. Carrillo-Conde BR, Brewer E, Lowman A, et al. Complexation Hydrogels as Oral Delivery Vehicles of Therapeutic Antibodies: An in Vitro and ex Vivo Evaluation of Antibody Stability and Bioactivity. Industrial & Engineering Chemistry Research. 2015 2015/10/28;54(42):10197–10205. doi: 10.1021/acs.iecr.5b01193.
35. Blanchette J, Kavimandan N, Peppas NA. Principles of transmucosal delivery of therapeutic agents. Biomedicine & Pharmacotherapy. 2004 2004/4/01/;58(3):142–151. doi: 10.1016/j.biopha.2004.01.006.
36. Liechty WB, Caldorera-Moore M, Phillips MA, et al. Advanced molecular design of biopolymers for transmucosal and intracellular delivery of chemotherapeutic agents and biological therapeutics. Journal of Controlled Release. 2011 2011/10/30/;155(2):119–127. doi: 10.1016/j.jconrel.2011.06.009.
37. Caldorera-Moore M, Peppas NA. Micro- and nanotechnologies for intelligent and responsive biomaterial-based medical systems. Advanced Drug Delivery Reviews. 2009 2009/12/17/;61(15):1391–1401. doi: 10.1016/j.addr.2009.09.002.
38. Peppas NA, Hilt JZ, Khademhosseini A, et al. Hydrogels in Biology and Medicine: From Molecular Principles to Bionanotechnology. Advanced Materials. 2006 2006/6/06;18(11):1345–1360. doi: 10.1002/adma.200501612.
39. Brannon-Peppas L, Peppas NA. Equilibrium swelling behavior of pH-sensitive hydrogels. Chemical Engineering Science. 1991 1991/1/01/;46(3):715–722. doi: 10.1016/0009-2509(91)80177-Z.
40. Brannon-Peppas L, Peppas NA. Time-dependent response of ionic polymer networks to pH and ionic strength changes. International Journal of Pharmaceutics. 1991 1991/3/31/;70(1):53–57. doi: 10.1016/0378-5173(91)90163-I.
41. Brannon-Peppas L, Peppas NA. Equilibrium swelling behavior of dilute ionic hydrogels in electrolytic solutions. Journal of Controlled Release. 1991 1991/8/01/;16(3):319–329. doi: 10.1016/0168-3659(91)90009-3.
42. Khare AR, Peppas NA. Swelling/deswelling of anionic copolymer gels. Biomaterials. 1995 1995/5/01/;16(7):559–567. doi: 10.1016/0142-9612(95)91130-Q.
43. Wood KM, Stone GM, Peppas NA. The effect of complexation hydrogels on insulin transport in intestinal epithelial cell models. Acta biomaterialia. 2010;6(1):48–56. [PubMed: 19481619]
44. Caldorera-Moore M, Maass K, Hegab R, et al. Hybrid responsive hydrogel carriers for oral delivery of low molecular weight therapeutic agents. Journal of Drug Delivery Science and Technology. 2015 2015/12/01/;30:352–359. doi: 10.1016/j.jddst.2015.07.023.
45. Lesuffleur T, Barbat A, Dussaulx E, et al. Growth Adaptation to Methotrexate of HT-29 Human Colon Carcinoma Cells Is Associated with Their Ability to Differentiate into Columnar Absorptive and Mucus-secreting Cells. Cancer Research. 1990;50(19):6334. [PubMed: 2205381]
46. Lesuffleur T, Porchet N, Aubert JP, et al. Differential expression of the human mucin genes MUC1 to MUC5 in relation to growth and differentiation of different mucus-secreting HT-29 cell subpopulations. Journal of Cell Science. 1993;106(3):771. [PubMed: 8308060]
47. Liechty WB, Scheuerle RL, Peppas NA. Tunable, responsive nanogels containing t-butyl methacrylate and 2-(t-butylamino)ethyl methacrylate. Polymer. 2013 2013/7/08/;54(15):3784–3795. doi: 10.1016/j.polymer.2013.05.045.

48. Puranik AS, Pao LP, White VM, et al. In Vitro Evaluation of pH-Responsive Nanoscale Hydrogels for the Oral Delivery of Hydrophobic Therapeutics. Industrial & Engineering Chemistry Research. 2016 2016/10/12;55(40):10576–10590. doi: 10.1021/acs.iecr.6b02565.
49. Zhou S, Sun J, Sun L, et al. Preparation and characterization of interferon-loaded magnetic biodegradable microspheres. Journal of Biomedical Materials Research Part B: Applied Biomaterials. 2008 2008/10/01;87B(1):189–196. doi: 10.1002/jbm.b.31091.
50. Delie F, Rubas W. A human colonic cell line sharing similarities with enterocytes as a model to examine oral absorption: advantages and limitations of the Caco-2 model. Crit Rev Ther Drug Carrier Syst. 1997;14(3):221–86. [PubMed: 9282267]
51. Hidalgo IJ, Raub TJ, Borchardt RT. Characterization of the human colon carcinoma cell line (Caco-2) as a model system for intestinal epithelial permeability. Gastroenterology. 1989 3;96(3): 736–49. [PubMed: 2914637]
52. Behrens I, Kissel T. Do cell culture conditions influence the carrier-mediated transport of peptides in Caco-2 cell monolayers? European Journal of Pharmaceutical Sciences. 2003 2003/8/01/;19(5): 433–442. doi: 10.1016/S0928-0987(03)00146-5.
53. Wikman A, Karlsson J, Carlstedt I, et al. A Drug Absorption Model Based on the Mucus Layer Producing Human Intestinal Goblet Cell Line HT29-H. Pharmaceutical Research. 1993 1993/6/01;10(6):843–852. doi: 10.1023/A:1018905109971.
54. Karlsson J, Wikman A, Artursson P. The mucus layer as a barrier to drug absorption in monolayers of human intestinal epithelial HT29-H goblet cells. International Journal of Pharmaceutics. 1993 1993/10/15/;99(2):209–218. doi: 10.1016/0378-5173(93)90363-K.
55. Meaney C, O'Driscoll C. Mucus as a barrier to the permeability of hydrophilic and lipophilic compounds in the absence and presence of sodium taurocholate micellar systems using cell culture models. European Journal of Pharmaceutical Sciences. 1999 1999/7/01/;8(3):167–175. doi: 10.1016/S0928-0987(99)00007-X.
56. Pontier C, Pachot J, Botham R, et al. HT29-MTX and Caco-2/TC7 monolayers as predictive models for human intestinal absorption: Role of the mucus layer. Journal of Pharmaceutical Sciences. 2001 2001/10/01;90(10):1608–1619. doi: 10.1002/jps.1111.
57. Walter E, Janich S, Roessler BJ, et al. HT29-MTX/Caco-2 cocultures as an in vitro model for the intestinal epithelium: In vitro–in vivo correlation with permeability data from rats and humans. Journal of Pharmaceutical Sciences. 1996 1996/10/01;85(10):1070–1076. doi: 10.1021/js960110x.
58. Pan F, Han L, Zhang Y, et al. Optimization of Caco-2 and HT29 co-culture in vitro cell models for permeability studies. International Journal of Food Sciences and Nutrition. 2015 2015/8/18;66(6): 680–685. doi: 10.3109/09637486.2015.1077792.
59. Srinivasan B, Kolli AR, Esch MB, et al. TEER measurement techniques for in vitro barrier model systems. Journal of laboratory automation. 2015;20(2):107–126. doi: 10.1177/2211068214561025. [PubMed: 25586998]
60. Ferraretto A, Bottani M, De Luca P, et al. Morphofunctional properties of a differentiated Caco2/ HT-29 co-culture as an in vitro model of human intestinal epithelium. Bioscience reports. 2018;38(2):BSR20171497. doi: 10.1042/BSR20171497. [PubMed: 29540534]
61. Sadeghi AMM, Dorkoosh FA, Avadi MR, et al. Permeation enhancer effect of chitosan and chitosan derivatives: Comparison of formulations as soluble polymers and nanoparticulate systems on insulin absorption in Caco-2 cells. European Journal of Pharmaceutics and Biopharmaceutics. 2008 2008/9/01/;70(1):270–278. doi: 10.1016/j.ejpb.2008.03.004.
62. Béduneau A, Tempesta C, Fimbel S, et al. A tunable Caco-2/HT29-MTX co-culture model mimicking variable permeabilities of the human intestine obtained by an original seeding procedure. European Journal of Pharmaceutics and Biopharmaceutics. 2014 2014/7/01/;87(2):290–298. doi: 10.1016/j.ejpb.2014.03.017.

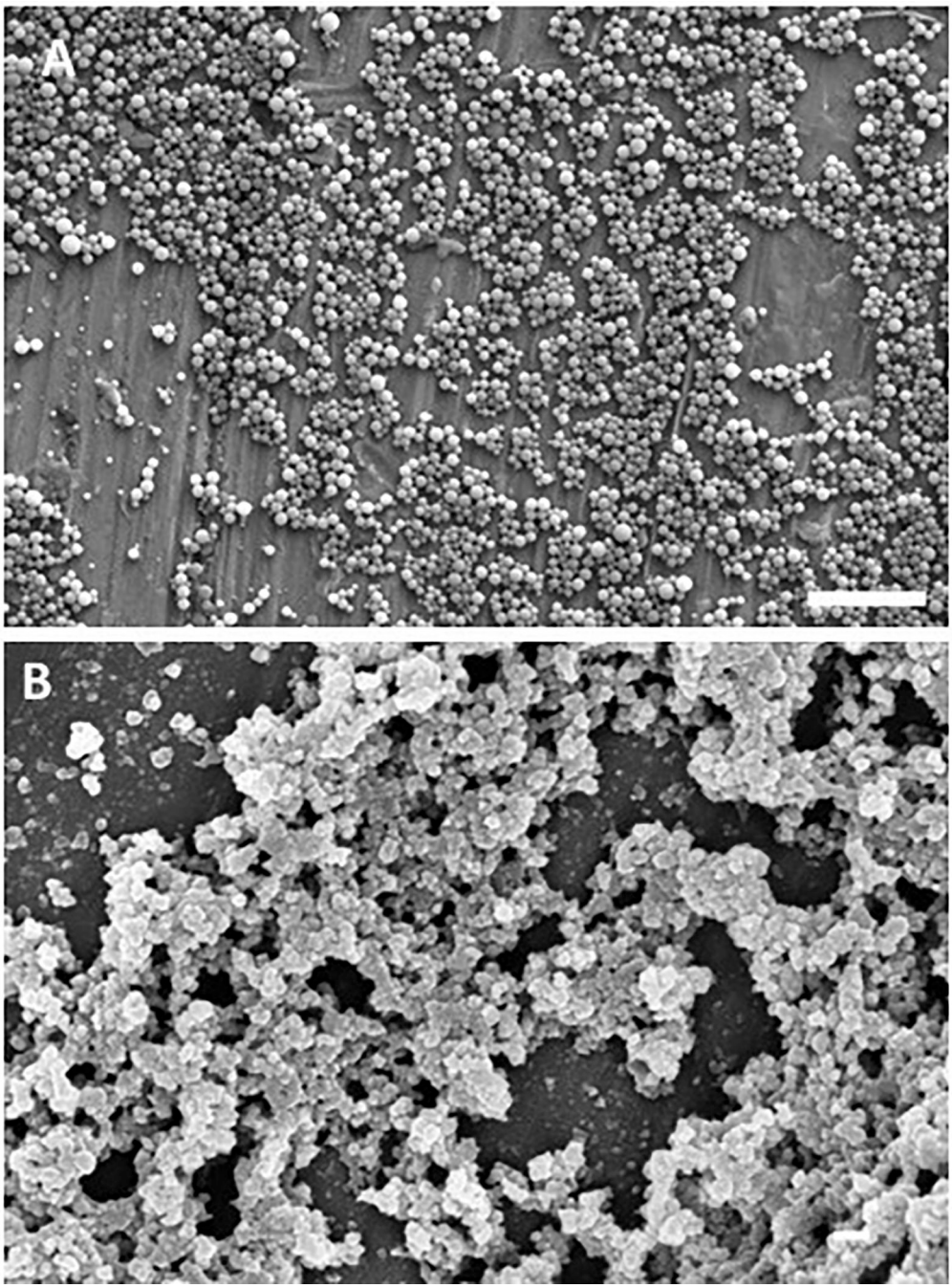

Figure 1: Scanning Electron Microscopy (SEM) of synthesized P(MAA-g-EG-co-tBMA) nanoparticles.

A) particles after synthesis, purification and dialysis, 10 μm scale bar and B) particles after freeze-dried, 200 nm scale bar.

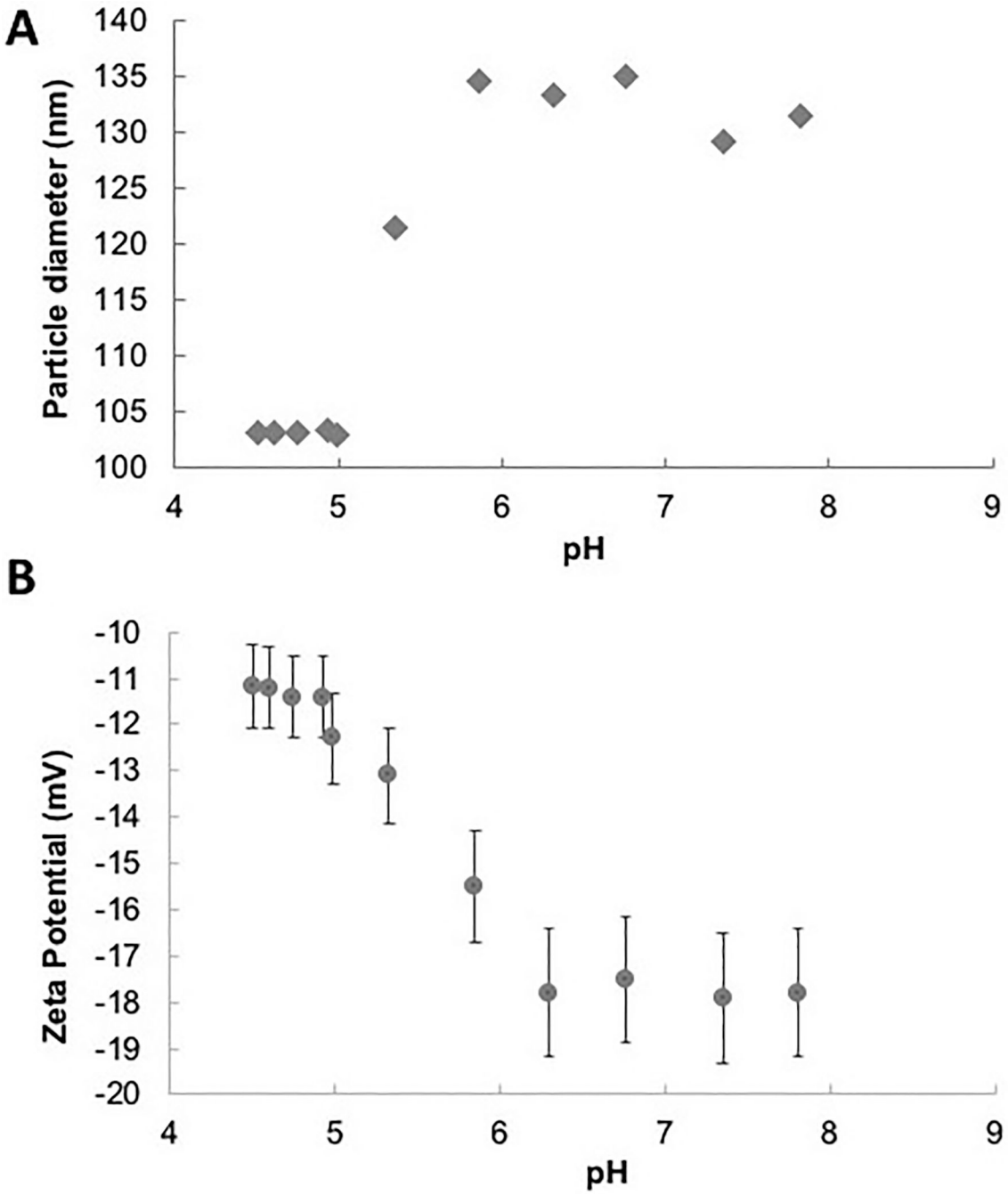

Figure 2: Dynamic Light Scattering (DLS) of synthesized P(MAA-g-EG-co-tBMA) nanoparticles.

A) particles average diameter as a function of pH, and B) nanoparticles zeta potential as a function of pH. Results are plots as average value of 3 runs with error bars being standard error.

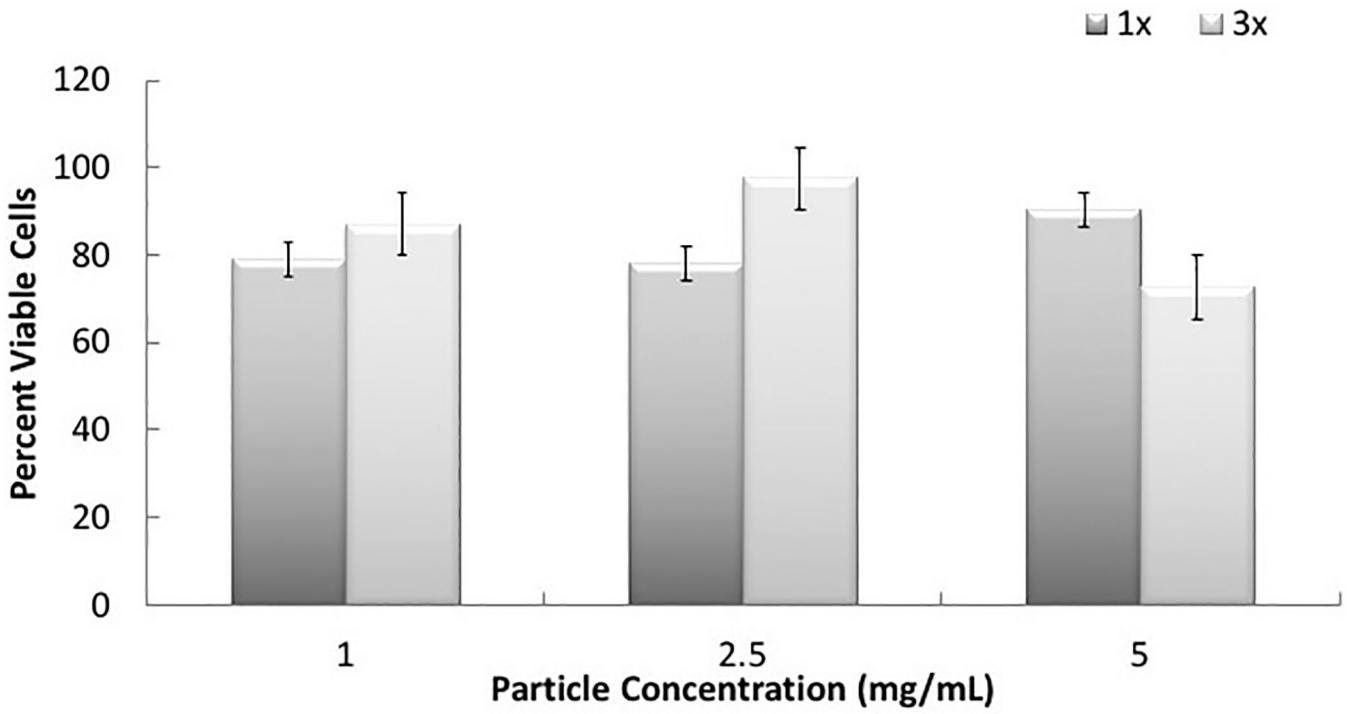

Figure 3: Viability of P(MAA-g-EG-co-tBMA) nanocarriers.

Percent viable cells as a function of total particle concentration exposed to Caco-2 and normalized to control cells, n=5 for each condition. The results show the effects by the P(MAA-g-EG-co-*t*BMA) nanoparticles with 1% (w/w) TEGDMA crosslinker (1X) and 3% (w/w) TEGDMA crosslinker (3X) at 1, 2.5 and 5 mg/mL concentrations.

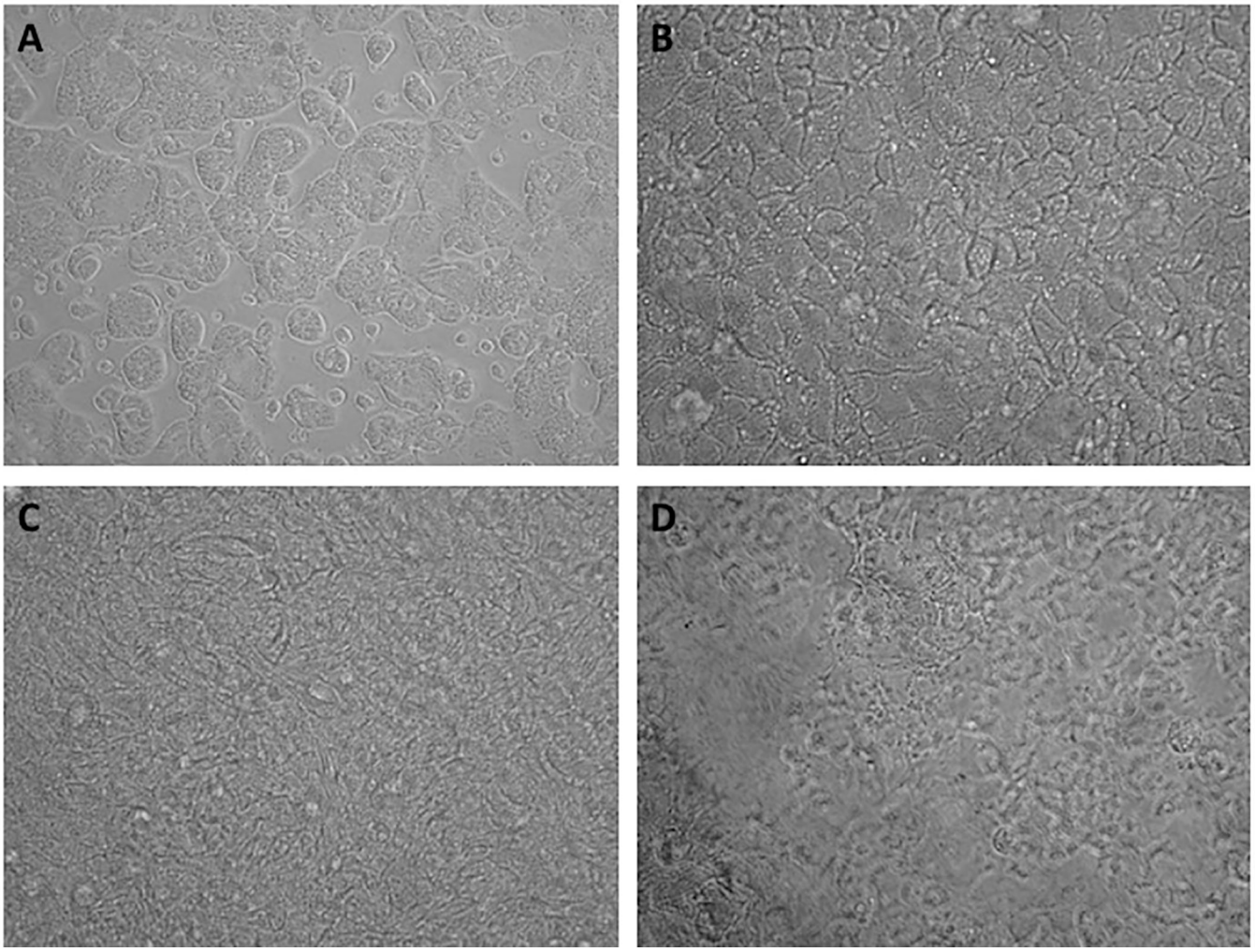

Figure 4: GI tract model: Caco-2/HT29-MTX co-culture over time.

Phase contrast images for Caco-2 and HT29-MTX co-culture at A) 72 hours, B) 7 days, C) 14 days and D) 21 days after seeding. Cells were seeded at a 1:1 cell ratio and were cultured for 24 days before transport studies were performed.

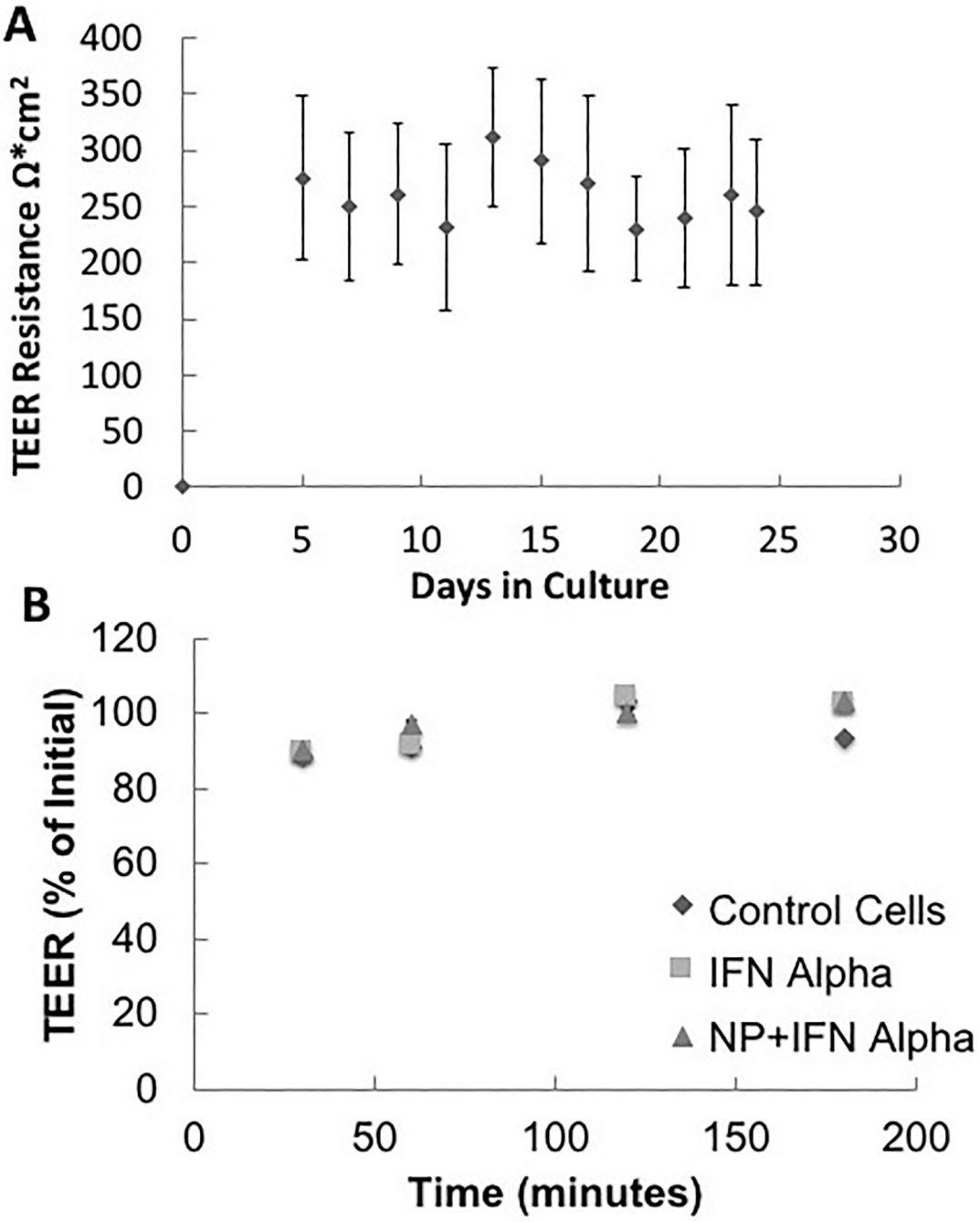

Figure 5: TEER values of Caco-2/HT29-MTX co-culture

A) over the 24 days growth period (n=24) and B) during transport studies experiments (n=4 for each condition). TEER studies monitor the electrical resistance of the developing cell layer with tight junctions; representative of intestinal lining

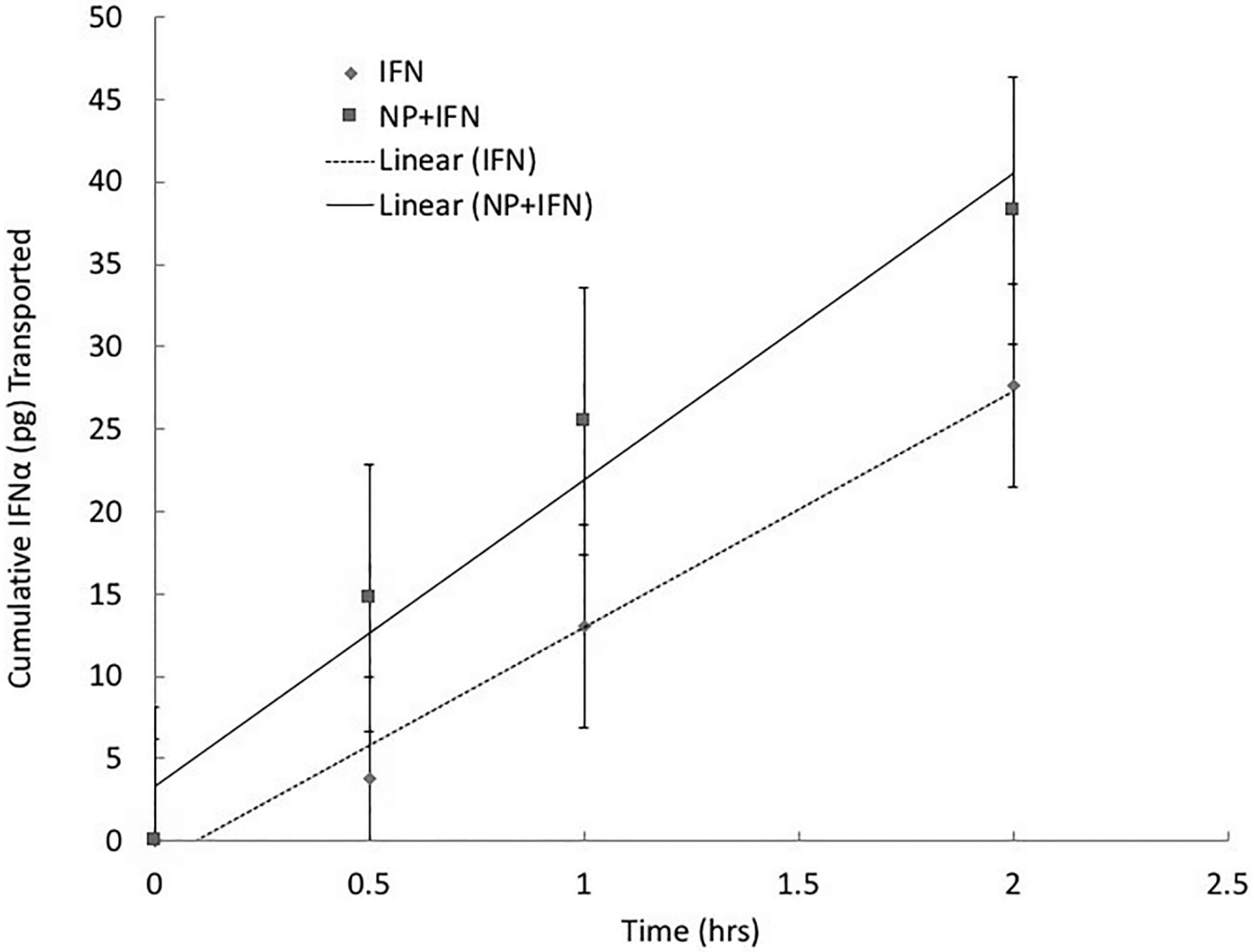

Figure 6: Cumulative IFN-α (pg) transported across Caco-2/HT29-MTX monolayer over time.
Results are presented as average and standard deviation.

Table 1:

IFN-α loading efficiency

	Amount Loaded (pg)	% Loaded
1 Hour	166.0 ± 68.4	60.4
After Particles Collapsed	156.7 ± 62.7	57.0
After Rinsing	103.6 ± 11.6	37.4

Table 2:

Permeability values for IFN-α transport in Caco-2/HT29-MTX monolayer

Formulation	$P_{app} \times 10^5$ (cm/s)
IFN-α	8.11 ± 1.8
IFN-α + Nanoparticles	9.36 ± 0.11